View metadata, citation and similar papers at core.ac.uk

brought to you by CORE

provided by Open Research Exeter

The Astrophysical Journal, 806:270 (10pp), 2015 June 20 doi:10.1088/0004-637X/806/2/270

© 2015. The American Astronomical Society. All rights reserved.

# THERMAL-GRAVITATIONAL WIND EQUATION FOR THE WIND-INDUCED GRAVITATIONAL SIGNATURE OF GIANT GASEOUS PLANETS: MATHEMATICAL DERIVATION, NUMERICAL METHOD, AND ILLUSTRATIVE SOLUTIONS

Keke Zhang[1], Dali Kong[2,3], and Gerald Schubert[4]

[1] Center for Geophysical and Astrophysical Fluid Dynamics and Department of Mathematical Sciences, University of Exeter, Exeter, EX4 4QF, UK; K.Zhang@exeter.ac.uk

[2] Center for Geophysical and Astrophysical Fluid Dynamics, University of Exeter, Exeter, EX4 4QF, UK

[3] Key Laboratory of Planetary Sciences, Chinese Academy of Sciences, Shanghai 200030, China; D.Kong@exeter.ac.uk

[4] Department of Earth, Planetary and Space Sciences, University of California, Los Angeles, CA 90095-1567, USA; schubert@ucla.edu

*Received 2015 February 26; accepted 2015 May 4; published 2015 June 23*

## ABSTRACT

The standard thermal wind equation (TWE) relating the vertical shear of a flow to the horizontal density gradient in an atmosphere has been used to calculate the external gravitational signature produced by zonal winds in the interiors of giant gaseous planets. We show, however, that in this application the TWE needs to be generalized to account for an associated gravitational perturbation. We refer to the generalized equation as the thermal-gravitational wind equation (TGWE). The generalized equation represents a two-dimensional kernel integral equation with the Green's function in its integrand and is hence much more difficult to solve than the standard TWE. We develop an extended spectral method for solving the TGWE in spherical geometry. We then apply the method to a generic gaseous Jupiter-like object with idealized zonal winds. We demonstrate that solutions of the TGWE are substantially different from those of the standard TWE. We conclude that the TGWE must be used to estimate the gravitational signature of zonal winds in giant gaseous planets.

*Key words:* planetary systems – planets and satellites: gaseous planets – planets and satellites: interiors

## 1. INTRODUCTION

Earth's atmosphere is a thin gaseous envelope held by the gravitational force primarily originating from its deep mantle and core. In the dynamics of the atmosphere, the thermal wind equation (TWE) is widely used to describe a relationship between the vertical shear of a wind and the corresponding horizontal gradient in density (see, e.g., Holton 2004). On the basis of the TWE, a diagnostic relation, one can estimate, if the vertical profile of velocity is known, the density profile by performing a simple integration over the horizontal coordinate.

The TWE has recently been used to compute the wind-induced density anomaly in the deep interiors of Jupiter, Saturn, Uranus, and Neptune and the corresponding external gravitational signatures (Kaspi et al. 2010, 2013; Kaspi 2013; Liu et al. 2013). The computed gravitational signatures, in turn, will be used to interpret the high-precision measurements of the external gravitational fields of Jupiter and Saturn to be carried out by the *Juno* and *Cassini* spacecraft.

The external gravitational potential $V_g$ of a giant planet, assuming that it is axially symmetric with respect to its rotation axis, can be expanded in terms of the Legendre functions $P_n$,

$$V_g = -\frac{GM}{r}\left[1 - \sum_{n=2}^{\infty} J_n \left(\frac{R_e}{r}\right)^n P_n(\cos\theta)\right], \quad (1)$$

for $r \geqslant R_e$, where $M$ is the mass of the planet, $(r, \theta, \phi)$ are spherical polar coordinates with the corresponding unit vectors $(\hat{\boldsymbol{r}}, \hat{\boldsymbol{\theta}}, \hat{\boldsymbol{\phi}})$, $\theta = 0$ is at the axis of rotation, $r = 0$ is located at the center of mass, $R_e$ is the equatorial radius, $n$ takes positive integer values, $J_2, J_3, J_4, \ldots$, are the zonal gravitational coefficients, and $G = 6.67384 \times 10^{-11}\,\mathrm{m^3\,kg^{-1}\,s^{-2}}$ is the universal gravitational constant. By assuming that the rotational effect on the shape of Jupiter is small and that the observed cloud-level zonal winds extend on cylinders parallel to the rotation axis into the deep interior, Kaspi et al. (2010) solved the TWE to estimate the wind-induced density anomaly and the corresponding gravitational correction $\Delta J_n^{\mathrm{dyn}}$ with $n$ even and $n \geqslant 2$ (see also Liu et al. 2013). The interpretation of these even-order gravitational coefficients is complicated by the rotational distortion that makes a leading-order contribution to the even gravitational coefficients $J_n$ with $2 \leqslant n \leqslant 10$ (Hubbard 2013; Kong et al. 2013a). Accordingly, Kaspi (2013), on the basis of a model of the equatorially antisymmetric zonal winds in the deep interiors of Jupiter and Saturn, also solved the TWE to compute the more readily interpretable odd zonal gravitational coefficients $J_n$ with $n \geqslant 3$ in Equation (1). A similar analysis was extended to estimate the penetration depth of the cloud-level zonal winds into the interiors of Uranus and Neptune (Kaspi et al. 2013).

Adoption of the TWE for the computation of the wind-induced gravitational signature originating from the deep interior of a giant gaseous planet is based on the following. Suppose first that the gaseous planet rotates uniformly about its symmetry $z$-axis with an angular velocity $\Omega\hat{\boldsymbol{z}}$ and is in hydrostatic equilibrium under the balance of a self-gravitational force $\boldsymbol{g}_{\mathrm{static}}(r, \theta)$ resulting from the hydrostatic density distribution $\rho_{\mathrm{static}}(r, \theta)$, the internal pressure gradient $\nabla p_{\mathrm{static}}(r, \theta)$, and the centrifugal force (Zharkov & Trubitsyn 1978). When the planetary shape and its internal density distribution $\rho_{\mathrm{static}}(r, \theta)$ are known, the corresponding gravitational force $\boldsymbol{g}_{\mathrm{static}}(r, \theta)$ and the even zonal gravitational coefficients $J_n^{\mathrm{static}}$ with $n \geqslant 2$ can be computed (Hubbard 2013; Kong et al. 2013b). Suppose now that the rotating gaseous planet also possesses a strong steady zonal wind $\boldsymbol{u}(r, \theta)$ in its deep interior. In this case, the interior hydrostatic density $\rho_{\mathrm{static}}(r, \theta)$ is slightly perturbed by the effect of the deep flow

with the total density given by $\rho = \rho_{\rm static} + \rho'$, where the standard TWE is used to link the wind-induced density $\rho'(r, \theta)$ to the deep zonal winds $\boldsymbol{u}(r, \theta)$ without accounting for the associated gravitational perturbation. The observed zonal gravitational coefficients $J_n$ in Equation (1) would comprise the two parts

$$J_n = J_n^{\rm static} + \Delta J_n^{\rm dyn},$$

where $J_n^{\rm static}$ is caused by the effect of rotational distortion while $\Delta J_n^{\rm dyn}$ is produced by the wind-induced density anomaly $\rho'(r, \theta)$. The gravitational coefficients $J_n$ thus provide an important constraint on the internal dynamics and structure of a rotating giant gaseous planet. Upon assuming that the effect of rotational distortion is negligibly small and that the gravitational perturbation associated with the density perturbation $\rho'(r, \theta)$ is also negligibly small, one can, for a given deep zonal wind $\boldsymbol{u}(r, \theta)$, readily solve the TWE in spherical geometry for $\rho'(r, \theta)$ and then determine the corresponding gravitational anomaly $\Delta J_n^{\rm dyn}$ (see, for example, Kaspi et al. 2010).

The mathematics behind use of the TWE is particularly simple (see, e.g., Kaspi et al. 2013). Suppose that the non-spherical effect can be neglected such that $J_n = \Delta J_n^{\rm dyn}$ in Equation (1). It follows that the spherically symmetric hydrostatic density $\rho_{\rm static}(r)$ and the associated gravitational force $\boldsymbol{g}_{\rm static}(r)$—where $\boldsymbol{g}_{\rm static}(r)$ can be readily computed from $\rho_{\rm static}(r)$—are related to the deep zonal winds $\boldsymbol{u}(r, \theta) = U(r, \theta)\hat{\boldsymbol{\phi}}$ and the wind-induced density $\rho'(r, \theta)$ through the differential form of the TWE

$$-2(\Omega\hat{\boldsymbol{z}}) \cdot \boldsymbol{\nabla}\left(\rho_{\rm static} U\hat{\boldsymbol{\phi}}\right) = \boldsymbol{\nabla}\rho' \times \boldsymbol{g}_{\rm static}. \quad (2)$$

Kaspi et al. (2010) used the density profile $\rho_{\rm static}(r)$ from an interior model given by Guillot & Morel (1995) to compute the corresponding gravitational force $\boldsymbol{g}_{\rm static}(r)$ for Jupiter. By integrating the azimuthal component of Equation (2) over $\theta$, an integral form of the TWE for the wind-induced density perturbation $\rho'(r, \theta)$ is obtained:

$$\rho' = C(r) + \frac{2r\Omega}{g_{\rm static}(r)} \int_{\pi/2}^{\theta} \left[\cos\tilde{\theta}\frac{\partial}{\partial r}\left(\rho_{\rm static} U\right) - \frac{\sin\tilde{\theta}}{r}\frac{\partial}{\partial\tilde{\theta}}\left(\rho_{\rm static} U\right)\right] d\tilde{\theta}, \quad (3)$$

where $\boldsymbol{g}_{\rm static} = \hat{\boldsymbol{r}} g_{\rm static}(r)$, $C(r)$ denotes an arbitrary function of $r$, and the second term on the right-hand side will be referred to as the wind-driving term. After computing the density perturbation $\rho'(r, \theta)$ using Equation (3) with a given $U(r, \theta)$, $\rho_{\rm static}(r)$, and $g_{\rm static}(r)$, the dynamic part of the gravitational coefficients $\Delta J_n^{\rm dyn}$ can be computed by performing a simple integration:

$$\Delta J_n^{\rm dyn} = \frac{-2\pi}{MR_{\rm s}^n} \int_0^{\pi} \int_0^{R_{\rm s}} r^{n+2}\rho' \sin\theta P_n \, dr \, d\theta. \quad (4)$$

where $R_{\rm s}$ is the radius of a spherical planet. It is well known that the solution of the TWE (3) is mathematically non-unique. An intricate mathematical property, as pointed out by Kaspi et al. (2010), is that, although the TWE cannot determine the wind-induced density distribution $\rho'(r, \theta)$, it can uniquely determine the gravitational coefficients $\Delta J_n^{\rm dyn}$ in spherical geometry because

$$\int_0^{\pi} \int_0^{R_{\rm s}} C(r) P_n(\cos\theta) \, r^{n+2} \sin\theta \, dr \, d\theta = 0,$$

for $n = 2, 3, 4, \ldots$. It is this special mathematical simplicity of the TWE given by Equation (3) that has led to its wide application for linking the zonal winds $U(r, \theta)\hat{\boldsymbol{\phi}}$ to the dynamic density perturbation $\rho'(r, \theta)$ in the deep interiors of giant gaseous planets.

The primary purpose of the present study is to show, via both mathematical analysis and the numerical computation of simple models, that the TWE given by Equation (3) is, in general, not valid for determining the density perturbation $\rho'(r, \theta)$ induced by zonal winds. We point out first that zonal flow produces not only the density perturbation $\rho'$ but also a concomitant gravitational perturbation $\boldsymbol{g}'(r, \theta)$ to the hydrostatic gravitational force $\boldsymbol{g}_{\rm static}$. In terms of the mathematical formulation, an extra term representing the gravitational perturbation $\boldsymbol{g}'$ produced by the interior density perturbation $\rho'$ is of the same order of magnitude as the term $\boldsymbol{\nabla}\rho' \times \boldsymbol{g}_{\rm static}$ in Equation (2) and, hence, must be retained. We then show that retaining the gravitational perturbation $\boldsymbol{g}'$ leads to the thermal-gravitational wind equation (TGWE), a two-dimensional kernel integral equation that, in contrast to the TWE (3), is much more difficult to solve. Through an analytical model for $\rho_{\rm static}(r)$ in spherical geometry, we demonstrate that solutions of the TGWE are substantially different from those of the TWE and that the TWE, in general, cannot provide a reasonable approximation to the TGWE.

It should be pointed out that the approach using the TWE or the TGWE is profoundly different from another approach that makes the barotropic assumption—the density $\rho$ in fully compressible gaseous planets is a function only of the pressure $p$. The barotropic model was adopted to study the effect of deep zonal winds on Jupiter's gravitational harmonics in spherical geometry (Hubbard 1999) and in non-spherical geometry (Kong et al. 2013a, 2014). There are at least four significant differences between the two different approaches. First, the TWE or TGWE model for computing the gravitational coefficients $\Delta J_n^{\rm dyn}$ has to adopt spherical geometry, while the barotropic model can be either spherical or non-spherical geometry. Second, the TWE or the TGWE represents a diagnostic relation and does not require any boundary condition for a solution of the density perturbation $\rho'(r, \theta)$. But an appropriate boundary condition for $\rho'(r, \theta)$ is required in solving the governing equations for the barotropic model. Third, both the density perturbation $\rho'(r, \theta)$ and the gravitational coefficients $\Delta J_n^{\rm dyn}$ can be uniquely determined for the barotropic model in spherical geometry or non-spherical geometry. With the TWE or TGWE model, however, while the gravitational coefficients $\Delta J_n^{\rm dyn}$ can be uniquely determined in spherical geometry, the density perturbation $\rho'(r, \theta)$ is always non-unique. Finally, a direct consequence of using the barotropic assumption is that

$$2(\Omega\hat{\boldsymbol{z}}) \cdot \boldsymbol{\nabla}\left(U(r, \theta)\hat{\boldsymbol{\phi}}\right) = \boldsymbol{\nabla}\left(\frac{1}{\rho}\right) \times \boldsymbol{\nabla}p(\rho) = 0.$$

This means that the azimuthal zonal winds $U(r, \theta)$ must be constant on cylinders parallel to the rotation axis, i.e.,

$\partial U/\partial z = 0$, where $z$ denotes the coordinate in the direction of rotation axis, which is consistent with the convection-driven zonal flow (see, e.g., Busse 1976; Zhang 1992; Zhang & Schubert 1996) and usually leads to an upper bound of the gravitational coefficients $\Delta J_n^{\rm dyn}$ (Hubbard 1999; Kong et al. 2012). The TWE or TGWE model is not restricted by the constant $U$ on cylinders and, hence, can introduce an extra parameter $H$ describing the radial penetration depth of the zonal winds $U$(see, e.g., Kaspi et al. 2010).

We begin by deriving the TGWE in Section 2 and then discussing a numerical method for solving the TGWE in spherical geometry in Section 3. With an analytical hydrostatic density $\rho_{\rm static}(r)$ together with a simple analytical profile of the deep zonal flow $\boldsymbol{u}$, we solve both the TWE and TGWE using exactly the same model in Section 4, demonstrating that the gravitational perturbation term neglected in the TWE (3) does indeed make a leading-order contribution. The paper closes with a summary and some remarks in Section 5.

## 2. DERIVATION OF THE TGWE

As in previous models (Kaspi et al. 2010, 2013; Kaspi 2013), ours also assumes that (i) giant gaseous planets with mass $M$ are isolated and rotating about the $z$-axis with angular velocity $\Omega\hat{\boldsymbol{z}}$, (ii) the planets are axially symmetric and consist of fully compressible gases, (iii) the zonal winds $\boldsymbol{u}$ observed at the cloud level represent a manifestation of the flow taking place in the deep interiors of the planets, (iv) the Rossby number of the zonal winds is small and both the viscous and magnetic effects are weak, and (v) the gaseous planets are in a statistically steady state. We are not interested in the special case when the zonal winds are largely confined to a very top thin layer of the stably stratified atmosphere because the mathematical problem is trivial and the winds have no measurable external gravitational signature.

The above assumptions lead to the following governing equations in the rotating frame of reference (Kaspi et al. 2013):

$$2\Omega\hat{\boldsymbol{z}}\times\boldsymbol{u} = -\frac{1}{\rho}\nabla p + \boldsymbol{g} + \frac{\Omega^2}{2}\nabla\left|\hat{\boldsymbol{z}}\times\boldsymbol{r}\right|^2, \tag{5}$$

$$\nabla\cdot(\boldsymbol{u}\rho) = 0, \tag{6}$$

where $\boldsymbol{u}(\boldsymbol{r})$ represents the velocity of the zonal winds, $\boldsymbol{r}$ denotes the position vector with the origin at the center of figure, $p(\boldsymbol{r})$ is the pressure, and $\rho(\boldsymbol{r})$ is the density. Equations (5) and (6), togeher with a given zonal flow $\boldsymbol{u}$, are to be solved subject to the two boundary conditions

$$p = 0, \tag{7}$$

$$V_{\rm g} + V_{\rm c} = \text{constant} \tag{8}$$

at the bounding surface $\mathcal{S}$ of the planet described by

$$r = \widetilde{R}(\theta),$$

where $V_{\rm c}$ is the centrifugal potential and $V_{\rm g}$ is the gravitational potential.

Suppose that the speed of the zonal flow $\boldsymbol{u}$ is small compared to the rotation speed of the planet,

$$\frac{U_0}{\Omega R_{\rm e}} \ll 1,$$

where $U_0$ is the typical speed of $\boldsymbol{u}$. Equations (5) and (6) can then be solved by making use of the expansions

$$p = p_{\rm static}(r,\theta) + p'(r,\theta), \tag{9}$$

$$\rho = \rho_{\rm static}(r,\theta) + \rho'(r,\theta), \tag{10}$$

$$\boldsymbol{g} = \boldsymbol{g}_{\rm static}(r,\theta) + \boldsymbol{g}'(r,\theta), \tag{11}$$

where the leading-order solution ($p_{\rm static}$, $\rho_{\rm static}$, and $\boldsymbol{g}_{\rm static}$) represents the hydrostatic state of the rotating gaseous planet, while ($p'$, $\rho'$, $\boldsymbol{g}'$) denotes the perturbations arising from the effect of the zonal winds $\boldsymbol{u}$. As a consequence of the rotational distortion, $\boldsymbol{g}_{\rm static}$ and $\nabla\rho_{\rm static}$ have both radial and latitudinal components, i.e.,

$$\hat{\boldsymbol{\theta}}\cdot\boldsymbol{g}_{\rm static} \neq 0 \quad\text{and}\quad \hat{\boldsymbol{\theta}}\cdot\nabla\rho_{\rm static} \neq 0.$$

For a rapidly rotating planet, expansions (9)–(11) yield two problems that are mathematically coupled and inseparable. The leading-order problem determines the shape $r = \widetilde{R}(\theta)$ of a rotationally distorted planet, as well as the internal distribution $p_{\rm static}(r,\theta)$, $\rho_{\rm static}(r,\theta)$, and $\boldsymbol{g}_{\rm static}(r,\theta)$ (Hubbard 2013; Kong et al. 2013b). With the availability of the shape $r = \widetilde{R}(\theta)$ and the hydrostatic solution ($p_{\rm static}$, $\rho_{\rm static}$, $\boldsymbol{g}_{\rm static}$), the next-order problem can be solved to determine the perturbations $p'$, $\rho'$, and $\boldsymbol{g}'$ induced by the zonal winds (Kong et al. 2013a).

Substitution of the expansions (9)–(11) into (5)–(6) yields the leading-order problem governed by

$$\boldsymbol{0} = -\frac{1}{\rho_{\rm static}(r,\theta)}\nabla p_{\rm static}(r,\theta) + \boldsymbol{g}_{\rm static}(r,\theta) + \frac{\Omega^2}{2}\nabla\left|\hat{\boldsymbol{z}}\times\boldsymbol{r}\right|^2, \tag{12}$$

$$\boldsymbol{g}_{\rm static}(r,\theta) = 2\pi G\,\nabla\left[\int_0^{\pi}\int_0^{\widetilde{R}(\tilde{\theta})}\frac{\tilde{r}^2\rho_{\rm static}(\tilde{r},\tilde{\theta})}{|\boldsymbol{r}-\tilde{\boldsymbol{r}}|}\sin\tilde{\theta}\,d\tilde{r}\,d\tilde{\theta}\right], \tag{13}$$

subject to the boundary condition

$$0 = p_{\rm static}, \tag{14}$$

$$\text{constant} = \left[\int_0^{\pi}\int_0^{r}\frac{\tilde{r}^2\rho_{\rm static}(\tilde{r},\tilde{\theta})}{|\boldsymbol{r}-\tilde{\boldsymbol{r}}|}\sin\tilde{\theta}\,d\tilde{r}\,d\tilde{\theta} + \frac{\Omega^2}{4\pi G}\left|\hat{\boldsymbol{z}}\times\boldsymbol{r}\right|^2\right]_{r=\widetilde{R}(\theta)} \tag{15}$$

at the bounding surface $\mathcal{S}$ of the rotating planet, where $[f]_{r=\widetilde{R}(\theta)}$ denotes the evaluation of $f$ at the bounding surface $\mathcal{S}$ of the planet. With a given equation of state, Equations (12)–(13) can be solved to determine the shape of the planet $r = \widetilde{R}(\theta)$ and the density distribution $\rho_{\rm static}(\boldsymbol{r})$ and the gravitational force $\boldsymbol{g}_{\rm static}(r,\theta)$.

The next-order problem, which describes the density anomaly $\rho'$ induced by the deep zonal flow $\boldsymbol{u}$ and the concomitant gravitational perturbation $\boldsymbol{g}'$ directly produced by $\rho'$, is governed by the equations

$$2\rho_{\rm static}(\Omega\hat{\boldsymbol{z}}\times\boldsymbol{u}) = -\nabla p' + \boldsymbol{g}_{\rm static}\rho' + \boldsymbol{g}'\rho_{\rm static}, \tag{16}$$

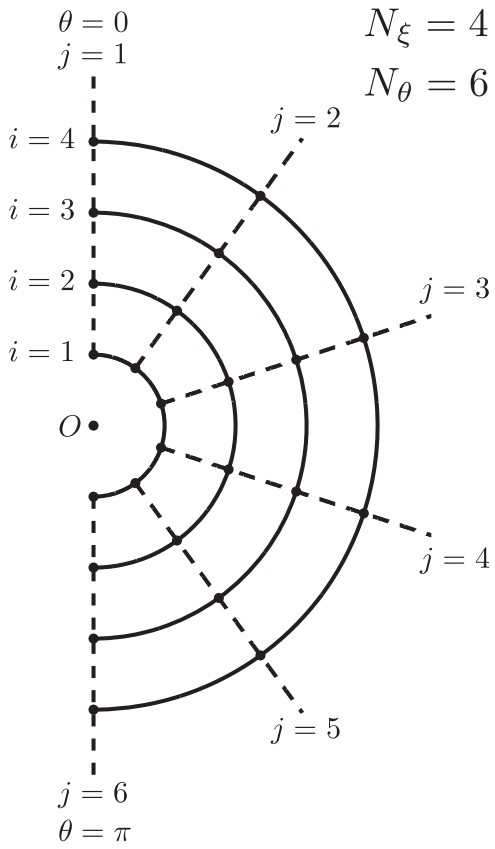


**Figure 1.** Schematic of the $r$–$\theta$ grid constructed in a meridional plane with $N_\xi = 4$ and $N_\theta = 6$. The radial grid points are numbered by index $i$ from 1 to $N_\xi$, while the angular grid points are labeled by index $j$ from 1 to $N_\theta$.

$$0 = \nabla \cdot (\boldsymbol{u}\rho_{\rm static}). \tag{17}$$

In deriving Equations (16) and (17), we have neglected the small high-order terms that are of $O(|\boldsymbol{g}'\rho'|)$ and $O(|\boldsymbol{u}\rho'\Omega|)$, and we have assumed that $\Omega$ is moderately small such that the term $(\rho'\Omega^2/2)\nabla\left|\hat{\boldsymbol{z}}\times\boldsymbol{r}\right|^2$ can be neglected. It is critically important to notice that the terms $\boldsymbol{g}_{\rm static}\rho'$ and $\boldsymbol{g}'\rho_{\rm static}$ in Equation (16) are generally of the same order of magnitude. This is because

$$\begin{aligned}&\left|\boldsymbol{g}_{\rm static}\rho'\right| \\ &\sim \left|\rho'\nabla\left[\int_0^\pi\int_0^{\tilde{R}(\tilde{\theta})}\frac{\tilde{r}^2\sin\tilde{\theta}\rho_{\rm static}}{|\boldsymbol{r}-\tilde{\boldsymbol{r}}|}\,d\tilde{r}\,d\tilde{\theta}\right]\right| \\ &= O\left(\rho'\rho_{\rm static}\right);\end{aligned} \tag{18}$$

$$\begin{aligned}&\left|\boldsymbol{g}'\rho_{\rm static}\right| \\ &\sim \left|\rho_{\rm static}\nabla\left[\int_0^\pi\int_0^{\tilde{R}(\tilde{\theta})}\frac{\tilde{r}^2\sin\tilde{\theta}\rho'}{|\boldsymbol{r}-\tilde{\boldsymbol{r}}|}\,d\tilde{r}\,d\tilde{\theta}\right]\right| \\ &= O\left(\rho'\rho_{\rm static}\right).\end{aligned} \tag{19}$$

Physically, it simply means that, when the internal density anomaly $\rho'$ is induced by the deep flow $\boldsymbol{u}$, the hydrostatic gravitational force $\boldsymbol{g}_{\rm static}$ must be also perturbed to yield the concomitant gravitational perturbation $\boldsymbol{g}'$.

Taking the curl of Equation (16), together with making use of Equation (17), we obtain

$$\begin{aligned}&-2(\Omega\hat{\boldsymbol{z}})\cdot\nabla(\rho_{\rm static}\boldsymbol{u}) \\ &\quad = \nabla\rho'\times\boldsymbol{g}_{\rm static}+\nabla\rho_{\rm static}\times\boldsymbol{g}',\end{aligned} \tag{20}$$

where $\hat{\boldsymbol{z}} = \hat{\boldsymbol{r}}\cos\theta - \hat{\boldsymbol{\theta}}\sin\theta$. With the zonal winds written as $\boldsymbol{u} = U(r,\theta)\hat{\boldsymbol{\phi}}$, the azimuthal component of Equation (20) can be expressed as

$$\begin{aligned}&-2\Omega\left[\cos\theta\frac{\partial}{\partial r}\left(\rho_{\rm static}U\right)-\frac{\sin\theta}{r}\frac{\partial}{\partial\theta}\left(\rho_{\rm static}U\right)\right] \\ &\quad = \hat{\boldsymbol{\phi}}\cdot\left[\nabla\rho'\times\boldsymbol{g}_{\rm static}+\nabla\rho_{\rm static}\times\boldsymbol{g}'\right],\end{aligned} \tag{21}$$

where $\rho_{\rm static}(r,\theta)$ and $\boldsymbol{g}_{\rm static}(r,\theta)$ are determined by the leading-order problem.

Solving Equation (21) to determine the density anomaly $\rho'(r,\theta)$ in non-spherical geometry is highly complicated. A drastic simplification (Kaspi et al. 2010, 2013; Kaspi 2013)—which is reasonable for understanding the wind-induced gravitational anomaly $J_n^{\rm dyn}$—can be made by assuming that the non-spherical effect is negligibly small, leading to the following approximations:

$$\begin{aligned}\rho_{\rm static}(r,\theta) &= \rho_{\rm static}(r),\\ \boldsymbol{g}_{\rm static}(r,\theta) &= g_{\rm static}(r)\hat{\boldsymbol{r}},\\ \nabla\rho_{\rm static}(r,\theta) &= q(r)\hat{\boldsymbol{r}},\\ \frac{dp_{\rm static}(r)}{dr} &= \rho_{\rm static}(r)g_{\rm static}(r),\\ \tilde{R}(\theta) &= R_{\rm s} = \text{constant},\end{aligned}$$

where $R_{\rm s}$ denotes the radius of a spherical planet. Note that the gravitational perturbation $\boldsymbol{g}'$ produced by the wind-induced density anomaly $\rho'(r,\theta)$ is generally two-dimensional in spherical geometry, i.e., $\hat{\boldsymbol{r}}\times\boldsymbol{g}'\neq\boldsymbol{0}$. It follows that Equation (21) in spherical geometry becomes

$$\begin{aligned}&2\Omega\left[\cos\theta\frac{\partial}{\partial r}\left(\rho_{\rm static}U\right)-\frac{\sin\theta}{r}\frac{\partial}{\partial\theta}\left(\rho_{\rm static}U\right)\right] \\ &\quad = \frac{g_{\rm static}(r)}{r}\frac{\partial\rho'}{\partial\theta}-\frac{2\pi Gq(r)}{r} \\ &\qquad\times\frac{\partial}{\partial\theta}\left[\int_0^\pi\int_0^{R_{\rm s}}\frac{\tilde{r}^2\rho'}{|\boldsymbol{r}-\tilde{\boldsymbol{r}}|}\sin\tilde{\theta}\,d\tilde{r}\,d\tilde{\theta}\right].\end{aligned} \tag{22}$$

Integrating Equation (22) over $\theta$ gives rise to

$$\begin{aligned}&2\Omega\int_{\pi/2}^\theta\left[\cos\tilde{\theta}\frac{\partial}{\partial r}-\frac{\sin\tilde{\theta}}{r}\frac{\partial}{\partial\tilde{\theta}}\right]\left(\rho_{\rm static}U\right)d\tilde{\theta} \\ &\quad = \frac{g_{\rm static}(r)}{r}\rho'(r,\theta)-\frac{2\pi Gq(r)}{r} \\ &\qquad\times\int_0^\pi\int_0^{R_{\rm s}}\frac{\tilde{r}^2\rho'\left(\tilde{r},\tilde{\theta}\right)}{|\boldsymbol{r}-\tilde{\boldsymbol{r}}|}\sin\tilde{\theta}\,d\tilde{r}\,d\tilde{\theta}+C(r),\end{aligned} \tag{23}$$

where $\boldsymbol{r} = \boldsymbol{r}(r,\theta)$, $\tilde{\boldsymbol{r}} = \tilde{\boldsymbol{r}}(\tilde{r},\tilde{\theta})$, and $C(r)$ is an arbitrary function of $r$. Since we are mainly concerned with the wind-induced gravitational anomaly $J_n^{\rm dyn}$, we set $C(r) = 0$ in Equation (23) without affecting the value of $J_n^{\rm dyn}$. For a given $U(r,\theta)$ and $\rho_{\rm static}(r)$, $g_{\rm static}(r)$ can be derived, and Equation

(23) can be solved for determining $\rho'(r, \theta)$, which can then be used to compute the wind-induced gravitational anomaly $J_n^{\rm dyn}$. Equation (23) represents a two-dimensional kernel integral equation, which in this paper will be referred to as TGWE. Finally, it should be noticed that

$$J_n^{\rm static} = 0, \quad n \geqslant 2,$$

since the non-spherical effect caused by rotation has been neglected.

Although the density anomaly $\rho'(r, \theta)$ represents a solution of the TGWE (23), we shall focus not on the actual profile of $\rho'(r, \theta)$ but, instead, on the distance $\Delta z$ between the center of mass and the center of figure and the wind-induced gravitational anomaly $J_n^{\rm dyn}$, which are derived using $\rho'(r, \theta)$ via the averaging process of a double integration. This is because both $\Delta z$ and $J_n^{\rm dyn}$ can be uniquely determined from the density anomaly $\rho'(r, \theta)$ in spherical geometry and have physical significance while a solution $[\mathcal{F}(r) + \rho'(r, \theta)]$, where $\mathcal{F}(r)$ is an arbitrary function, can be another solution of the TGWE. This non-uniqueness makes the precise structure of $\rho'(r, \theta)$ physically or mathematically less significant.

## 3. A METHOD FOR SOLVING THE TGWE

In contrast to the TWE (3), it is much more difficult to solve the two-dimensional kernel integral TGWE (23) that contains the Green's function $1/|\boldsymbol{r} - \tilde{\boldsymbol{r}}|$ in its integrand. We seek a numerical solution for the TGWE by employing an extended spectral method for which the $r$–$\theta$ grids in a meridional plane are illustrated in Figure 1. In the framework of the $r$–$\theta$ grid, it is mathematically convenient to define

$$\begin{aligned}
r_i &= \left(\frac{R_{\rm s}}{N_\xi}\right) i, \quad i = 1, 2, 3, ..., N_\xi;\\
\xi_i &= \frac{r_i}{\mathcal{L}}, \quad i = 1, 2, 3, ..., N_\xi;\\
\theta_j &= \left(\frac{\pi}{N_\theta - 1}\right)(j-1), \quad j = 1, 2, 3, ..., N_\theta;\\
\Phi_{ij} &= \Phi(r_i, \theta_j),
\end{aligned}$$

where $\Phi_{ij}$ denotes the function $\Phi$ evaluated at the grid point $r = r_i$ and $\theta = \theta_j$, and $\xi = r/\mathcal{L}$ is the dimensionless radial coordinate scaled by $\mathcal{L}$ whose choice depends on the hydrostatic state. We return to the scaling $\mathcal{L}$ in the next section.

The Green's function $1/|\boldsymbol{r} - \tilde{\boldsymbol{r}}|$ at the numerical grid point $(r_i, \theta_j)$ can be expanded as

$$\frac{1}{|\boldsymbol{r}_{ij} - \tilde{\boldsymbol{r}}_{lm}|} = \frac{1}{\mathcal{L}} \sum_{n=0}^{\infty} f_n(\xi_i, \tilde{\xi}_l) P_n(\cos\theta_j) P_n(\cos\tilde{\theta}_m), \quad (24)$$

where $P_n$ is the Legendre polynomial of order $n$ normalized by

$$\int_0^\pi P_n(\cos\theta) P_q(\cos\theta) \sin\theta \, d\theta = \frac{2}{2n+1}\delta_{nq},$$

and the function $f_n(\xi_i, \tilde{\xi}_l)$ is defined as

$$f_n(\xi_i, \tilde{\xi}_l) = \begin{cases} \tilde{\xi}_l^n / \xi_i^{n+1}, & \tilde{\xi}_l \leqslant \xi_i, \\ \xi_i^n / \tilde{\xi}_l^{n+1}, & \tilde{\xi}_l > \xi_i. \end{cases}$$

In contrast to an ordinary numerical integration, the grid point at $j = m$ and $i = l$ in expansion (24), because of the nature of the Green's function, must be treated in a special way.

In order to solve the TGWE (23) for the density anomaly $\rho'$ induced by a deep wind $U(r, \theta)$, we have to rewrite the kernel integral in terms of an appropriate quadrature scheme. Based on the $\xi$–$\theta$ grid system illustrated in Figure 1, the two-dimensional integral on the right-hand side of the TGWE (23) can be expressed as

$$\begin{aligned}
&\left\{\int_0^\pi \int_0^{R_{\rm s}} \frac{\tilde{r}^2 \rho'(\tilde{r}, \tilde{\theta})}{|\boldsymbol{r}(r, \theta) - \tilde{\boldsymbol{r}}(\tilde{r}, \tilde{\theta})|} \sin\tilde{\theta} \, d\tilde{r} \, d\tilde{\theta}\right\}_{ij}\\
&= -\mathcal{L}^2 \sum_{l=1}^{N_\xi} \sum_{m=1}^{N_\theta} \rho'_{lm} \tilde{\xi}_l^2 \sin\tilde{\theta}_m \Delta\theta w_\theta \Delta\xi w_\xi\\
&\quad \times \left[\sum_{n=0}^{\infty} f_n(\xi_i, \tilde{\xi}_l) P_n(\cos\theta_j) P_n(\cos\tilde{\theta}_m)\right], \quad (25)
\end{aligned}$$

where $N_\xi$ takes an even integer value, $\Delta\xi = R_{\rm s}/(\mathcal{L}N_\xi)$ denotes the radial grid spacing, $\Delta\theta = \pi/(N_\theta - 1)$ is the angular grid spacing, and $w_\xi$ and $w_\theta$ are the quadrature weight factors whose values depend on the locations of the grid points, which is discussed below.

Upon substituting Equation (25) into the TGWE (23), truncating the infinite spectral expansion in Equation (24) by replacing $\infty$ with $N$, and making the spatial discretization with the $\xi$–$\theta$ grid, we derive a system of numerical equations

$$\begin{aligned}
&\left\{\int_{\pi/2}^{\theta} \left[\cos\tilde{\theta}\frac{\partial}{\partial r} - \frac{\sin\tilde{\theta}}{r}\frac{\partial}{\partial\tilde{\theta}}\right](\rho_{\rm static} U) \, d\tilde{\theta}\right\}_{ij}\\
&= \frac{g_{\rm static}(r_i)}{2\Omega r_i}\rho'_{ij} - \frac{\pi G \mathcal{L}^2 q(r_i)}{\Omega r_i}\\
&\quad \times \sum_{l=1}^{N_\xi} \sum_{m=1}^{N_\theta} \rho'_{lm} \tilde{\xi}_l^2 \sin\tilde{\theta}_m \Delta\theta w_\theta \Delta\xi w_\xi\\
&\quad \times \left[\sum_{n=0}^{N} f_n(\xi_i, \tilde{\xi}_l) P_n(\cos\theta_j) P_n(\cos\tilde{\theta}_m)\right] \quad (26)
\end{aligned}$$

for $i = 1, 2, 3, \cdots, N_\xi$ and $j = 1, 2, 3, \cdots, N_\theta$. For a given $\rho_{\rm static}(r)$, the corresponding $g_{\rm static}(r)$ derived from $\rho_{\rm static}(r)$, and $U(r, \theta)$, Equation (26) gives rise to a system of the $N_\xi \times N_\theta$ linear equations that can be solved for the density anomaly $\rho'(r, \theta)$ whose numerical value is given at the $N_\xi \times N_\theta$ grid points.

The numerical quadrature in Equation (26) is, however, significantly complicated by the singular nature of the Green's function $1/|\boldsymbol{r} - \tilde{\boldsymbol{r}}|$ in the TGWE (23). Two different integration schemes must be adopted in evaluating the $\theta$-dimension quadrature in Equation (26). When $l \neq i$, an extended trapezoidal scheme is adopted by using the quadrature weight factors in the form

$$\begin{aligned}
w_\theta &= \frac{1}{2}, \quad m = 1 \text{ or } m = N_\theta,\\
w_\theta &= 1, \quad 1 < m < N_\theta.
\end{aligned}$$

When $l = i$, the rectangle rule is adopted in the neighborhood of $m = j$, which leads to the quadrature weight factors

$$\begin{aligned} w_\theta &= \frac{1}{2}, \quad m = 1 \text{ or } m = N_\theta; \\ w_\theta &= 1, \quad m = 2, 3, ..., (j-2); \\ w_\theta &= 0, \quad m = j; \\ w_\theta &= \frac{3}{2}, \quad m = (j-1), (j+1); \\ w_\theta &= 1, \quad m = (j+2), (j+3), ..., (N_\theta - 1) \end{aligned}$$

for $j > 3$ or $j < (N_\theta - 2)$. When $j \leqslant 3$ or $j \geqslant (N_\theta - 2)$, slightly different but similar weight factors would be adopted. In the radial direction, the central grid point at $\xi_0 = 0$ does not enter the problem, a consequence of the Jacobian $\xi^2 \sin\theta$ in the quadrature. We can use an extended Simpson quadrature in the radial direction with its weight factors $w_\xi$ given by

$$\begin{aligned} w_\xi &= \frac{1}{3}, \quad l = 0 \text{ or } l = N_\xi; \\ w_\xi &= \frac{2}{3}, \quad l \text{ is even}; \\ w_\xi &= \frac{4}{3}, \quad l \text{ is odd}. \end{aligned}$$

The resulting non-sparse system (26) can be solved numerically, for example, using a direct lower-upper decomposition method. The numerical convergence of the system (26) is expected to be slow because of the inherent numerical difficulties for the Green's function $1/|\boldsymbol{r} - \tilde{\boldsymbol{r}}|$ in the integrand.

## 4. ILLUSTRATIVE SOLUTIONS: TWE VERSUS TGWE

When using either the TWE (3) or the TGWE (23) to determine the wind-induced density perturbation $\rho'$, we require the density profile $\rho_{\text{static}}(r)$ for which there exists a family of planetary interior models. Since our primary purpose is to demonstrate that solutions of the TWE given by Equation (3), for the same $\rho_{\text{static}}(r)$, are generally substantially different from that of the TGWE (23), we choose a simple model for $\rho_{\text{static}}(r)$ and $U(r, \theta)$ such that the wind-driving term in both the TWE (3) and the TGWE (23) can be evaluated analytically.

When the effect of rotation upon the shape of a rotating planet is negligibly small, the hydrostatic Equations (12) and (13) become

$$\mathbf{0} = -\frac{1}{\rho_{\text{static}(r)}} \nabla p_{\text{static}}(r) + \boldsymbol{g}_{\text{static}}(r), \tag{27}$$

$$\boldsymbol{g}_{\text{static}}(r) = 2\pi G \nabla \left[ \int_0^\pi \int_0^{R_s} \frac{\tilde{r}^2 \rho_{\text{static}}(\tilde{r})}{|\boldsymbol{r} - \tilde{\boldsymbol{r}}|} \sin\tilde{\theta}\, d\tilde{r}\, d\tilde{\theta} \right], \tag{28}$$

subject to the boundary condition $p_{\text{static}} = 0$ at the spherical surface $r = R_s$. To derive an analytic solution for $\rho_{\text{static}}(r)$, we assume that the planetary interior in the hydrostatic state can be approximately described by a polytropic gas with index unity obeying the equation of state (Hubbard 1999)

$$p_{\text{static}} = K\, \rho_{\text{static}}^2, \tag{29}$$

where $K$ is a constant; this provides a reasonably good approximation for the interior of Jupiter (Hubbard 1999; Kong et al. 2013b). With this hydrostatic solution, we choose the radial scale $\mathcal{L}$ as

$$\mathcal{L} = \sqrt{\frac{K}{2\pi G}} \quad \text{and} \quad \xi = \frac{r}{\mathcal{L}} \quad \text{with} \quad 0 \leqslant \xi \leqslant \pi,$$

and, consequently, Equation (27) becomes

$$\frac{1}{\xi^2}\frac{d}{d\xi}\left[\xi^2 \frac{d(\rho_{\text{static}}/\rho_c)}{d\xi}\right] + \frac{\rho_{\text{static}}}{\rho_c} = 0, \tag{30}$$

where $\rho_c$ represents the central density. It is well known (see, e.g., Chandrasekhar 1933) that the solution $\rho_{\text{static}}(r)$ for Equation (30) is

$$\rho_{\text{static}}(r) = \frac{\rho_c \sin(r/\mathcal{L})}{(r/\mathcal{L})} = \frac{\rho_c \sin\xi}{\xi}. \tag{31}$$

An advantage of using Equation (31) is that analytic expressions for $q(r)$ and $g_{\text{static}}(r)$ in closed form can be derived. The radial derivative of $\rho_{\text{static}}$ is

$$q(r) = \frac{d\rho_{\text{static}}}{dr} = \left(\frac{\rho_c}{\mathcal{L}}\right)\frac{\xi\cos\xi - \sin\xi}{\xi^2}, \tag{32}$$

and Equation (28) gives rise to

$$\begin{aligned} g_{\text{static}}(r) &= (2\pi G)\hat{\boldsymbol{r}} \cdot \nabla \left[ \int_0^\pi \int_0^{R_s} \frac{\tilde{r}^2 \rho_{\text{static}}(\tilde{r})}{|\boldsymbol{r} - \tilde{\boldsymbol{r}}|} \sin\tilde{\theta}\, d\tilde{r}\, d\tilde{\theta} \right] \\ &= \left(4\pi \mathcal{L} G \rho_c\right)\frac{\xi\cos\xi - \sin\xi}{\xi^2}. \end{aligned} \tag{33}$$

In this case $g_{\text{static}}(r) = 2\,Kq(r)$. With the analytic expressions for $g_{\text{static}}(r)$ and $q(r)$ we are now in a position to solve either the TWE (3) or the TGWE (23) with a given zonal flow $U(r, \theta)$. Two different cases, equatorially symmetric and equatorially antisymmetric winds, will be considered.

Since the primary purpose of computing illustrative solutions is to demonstrate that the solution of the TGWE (23) differs substantially from that of the TWE (3) for exactly the same model and parameter values and, hence, the TWE cannot generally provide a reasonable approximation to the TGWE, we must find an effective way of measuring the difference between the TWE and TGWE solutions. We introduce three characteristic quantities for this purpose. First, we introduce the norm $\Delta_{\text{diff}}$ defined as

$$\Delta_{\text{diff}} = \frac{\| \rho'_{\text{TGWE}}(\boldsymbol{r}) - \rho'_{\text{TWE}}(\boldsymbol{r}) \|_2}{\| \rho'_{\text{TWE}}(\boldsymbol{r}) \|_2},$$

where the solution $\rho'$ of the TWE (3) is denoted as $\rho'_{\text{TWE}}$, the solution $\rho'$ of the TGWE (23) as $\rho'_{\text{TGWE}}$, and

$$\| F \|_2 = \left[ \int_0^{2\pi} \int_0^\pi \int_0^{R_s} |F(\boldsymbol{r})|^2 r^2 \sin\theta\, dr\, d\theta\, d\phi \right]^{1/2},$$

to measure the difference between $\rho'_{\text{TGWE}}$ and $\rho'_{\text{TWE}}$. The second characteristic quantity, adopted in the case of an equatorially antisymmetric wind, is the distance $\Delta z$ between

the center of mass and the center of figure caused by the wind-induced density anomaly. Although we can, in principle, compute $J_3$ using the known coordinate of the center of mass, comparing $(\Delta z)_{\rm TGWE}$ based on $\rho'_{\rm TGWE}$ to $(\Delta z)_{\rm TWE}$ based on $\rho'_{\rm TWE}$ suffices to serve our primary purpose. The third characteristic quantity, adopted in the case of an equatorially symmetric wind, is the lowermost coefficient $(J_2)_{\rm TGWE}$ computed from $\rho'_{\rm TGWE}$ and $(J_2)_{\rm TWE}$ from $\rho'_{\rm TWE}$. We believe that $\Delta_{\rm diff} = {\rm O}(100\%)$ together with

$$\frac{\left[(\Delta z)_{\rm TGWE} - (\Delta z)_{\rm TWE}\right]}{(\Delta z)_{\rm TWE}} = {\rm O}(100\%)$$

and

$$\frac{\left[(J_2)_{\rm TGWE} - (J_2)_{\rm TWE}\right]}{(J_2)_{\rm TWE}} = {\rm O}(100\%)$$

are sufficient to reconfirm the result of the order-of-magnitude analysis given by Equations (18) and (19): the gravitational perturbation term in the TGWE (23) neglected in the TWE (3) generally makes a leading-order contribution and, hence, must be retained.

### 4.1. Equatorially Antisymmetric Zonal Winds

First, consider the equatorially antisymmetric wind $U_{\rm asym}(r, \theta)$ in the form

$$U_{\rm asym} = U_0\left(\frac{r\sin\theta}{R_{\rm s}}\right)^2\left(\frac{r\cos\theta}{R_{\rm s}}\right)e^{-\frac{R_{\rm s}-r}{hR_{\rm s}}}, \tag{34}$$

where $U_0 = \Omega R_{\rm s}/100 = {\rm O}(100{\rm m/s})$ represents a typical speed of the zonal winds,

$$U_{\rm asym}(r, \theta) = -U_{\rm asym}(r, \pi - \theta),$$

and $h$ is the depth parameter. Using this simple wind profile (34), together with the simple interior density profile $\rho_{\rm static}(r)$ given by Equation (31), an explicit analytic expression for the wind-driving term in the TWE (3) or the TGWE (23) can be derived:

$$\begin{aligned}
&2\Omega\int_{\pi/2}^{\theta}\left[\cos\tilde\theta\frac{\partial}{\partial r} - \frac{\sin\tilde\theta}{r}\frac{\partial}{\partial\tilde\theta}\right]\left(\rho_{\rm static}U_{\rm asym}\right)d\tilde\theta\\
&\quad= \frac{\Omega^2\rho_{\rm c}}{50\pi^2}e^{-\frac{\pi-\xi}{h\pi}}\left[\left(\xi^2\cos\xi + \frac{1}{h\pi}\xi^2\sin\xi\right)\right.\\
&\qquad\times\left(\frac{\theta}{8} - \frac{\sin 4\theta}{32} - \frac{\pi}{16}\right)\\
&\qquad\left.+\ \xi\sin\xi\left(\frac{3\theta}{8} - \frac{\sin 2\theta}{4} + \frac{\sin 4\theta}{32} - \frac{3\pi}{16}\right)\right].
\end{aligned} \tag{35}$$

Using Equation (35), the numerical form of the TGWE (26) for the anti-equatorially symmetric zonal wind becomes

$$\begin{aligned}
&\frac{\Omega^2}{200\pi^3 G}e^{-\frac{\pi-\xi_i}{h\pi}}\left(\frac{\xi_i^4}{\xi_i\cos\xi_i - \sin\xi_i}\right)\\
&\quad\times\left[\left(\xi_i\cos\xi_i + \frac{1}{h\pi}\xi_i\sin\xi_i\right)\left(\frac{\theta_j}{8} - \frac{\sin 4\theta_j}{32} - \frac{\pi}{16}\right)\right.\\
&\quad\left.+\ \sin\xi_i\left(\frac{3\theta_j}{8} - \frac{\sin 2\theta_j}{4} + \frac{\sin 4\theta_j}{32} - \frac{3\pi}{16}\right)\right]\\
&\quad= \rho'_{ij} - \frac{1}{2}\sum_{l=1}^{N_\xi}\sum_{m=1}^{N_\theta}\sin\tilde\theta_m\rho'_{lm}\Delta\theta w_\theta\tilde\xi_l^{\,2}\Delta\xi w_\xi\\
&\qquad\times\sum_{n=0}^{N} f_n\left(\xi_i, \tilde\xi_l\right)P_n\left(\cos\theta_j\right)P_n\left(\cos\tilde\theta_m\right)
\end{aligned} \tag{36}$$

for $i = 1, 2, 3, \cdots, N_\xi$ and $j = 1, 2, 3, \cdots, N_\theta$. Since the parameters $R_{\rm s}$, $\Omega$, $\mathcal{L}$ appear as the same common factors in both the TWE (3) and the TGWE (23) and since our primary purpose is to show the difference between the solutions of Equations (3) and (23), we are free to select the parameters in Equation (36). For this reason, we consider a generic object whose parameter values are guided by those of Jupiter: $R_{\rm s} = 69{,}911$km, $\Omega = 1.7585\times10^{-4}\,{\rm s}^{-1}$, $\mathcal{L} = 22253$ km, and $M = 1.8986\times10^{27}$ kg.

It is important to note that solutions of Equation (36) give the wind-induced density anomaly $\rho'(r, \theta)$ obeying the equatorial parity

$$\rho'(r, \theta) = -\rho'(r, \pi - \theta).$$

As a consequence of this density parity, the center of mass for the gaseous planet would slightly shift from the center of figure along the axis of rotation. The distance $\Delta z$ between the center of mass and the center of figure can be calculated by the following integration:

$$\begin{aligned}
\Delta z &= \frac{1}{M}\int_0^{2\pi}\int_0^{\pi}\int_0^{R_{\rm s}}\left(\rho_{\rm static} + \rho'\right)\\
&\quad\times r^3\sin\theta\cos\theta\,dr\,d\theta\,d\phi\\
&= \frac{4\pi}{M}\int_0^{\pi/2}\int_0^{R_{\rm s}}\rho' r^3\sin\theta\cos\theta\,dr\,d\theta.
\end{aligned}$$

It follows that the center of mass in the presence of the equatorially antisymmetric wind (34) is located at $(\theta = 0, r = \Delta z)$ on the rotation axis.

We consider two different values for the depth parameter $h$ in the equatorially antisymmetric zonal wind $U_{\rm asym}(r, \theta)$ given by Equation (34) using the same $\rho_{\rm static}(r)$ given by Equation (31) and the same $g_{\rm static}(r)$ given by Equation (33). It is found that, for a large depth parameter $h = 1.1430$ with the parameters of the generic object, the difference between $\rho'_{\rm TGWE}$ and $\rho'_{\rm TWE}$ is

$$\Delta_{\rm diff} = \frac{\|\rho'_{\rm TGWE}(\boldsymbol{r}) - \rho'_{\rm TWE}(\boldsymbol{r})\|_2}{\|\rho'_{\rm TWE}(\boldsymbol{r})\|_2} = 90.26\%.$$

**Table 1**
The Numerical Behavior of Convergence for the System (36) for Two Different Depth Parameters $h = 0.1430$ and $h = 1.1430$ for $N = 50$

| $N_\xi \times N_\theta$ | $(\Delta z)_{h=1.1430}$ (km) | $(\Delta z)_{h=0.1430}$ (km) |
|---|---|---|
| 100 × 200 | −15.94 | −4.25 |
| 120 × 240 | −10.36 | −2.96 |
| 140 × 280 | −8.58 | −2.54 |
| 160 × 320 | −7.73 | −2.34 |
| 180 × 360 | −7.24 | −2.22 |
| 200 × 400 | −6.92 | −2.15 |
| 220 × 440 | −6.71 | −2.06 |

For the distance $\Delta z$ between the center of mass and the center of figure, the solution $\rho'_{\rm TGWE}$ of Equation (36) yields

$$(\Delta z)_{\rm TGWE} = -6.56\ {\rm km},$$

while the solution $\rho'_{\rm TWE}$ of the TWE (3) gives

$$(\Delta z)_{\rm TWE} = -1.13\ {\rm km}$$

for exactly the same model and parameter values. The value of $(\Delta z)_{\rm TGWE}$ is nearly six times larger compared to $(\Delta z)_{\rm TWE}$. The above numbers, because of the unrealistic wind profile (34), do not have much physical significance. But it has an important mathematical significance: the TGWE (23) is profoundly different from the TWE (3), and the TWE (3) does not generally provide a reasonable approximation to the TGWE (23). The large difference between the solutions of (3) and (23) is obviously attributed to the fact that the gravitational perturbation, represented by the second term on the right-hand side of Equation (23) and directly caused by the wind-induced density perturbation, which is neglected in the TWE (3), is the same order of magnitude as the first term on the right-hand side of Equation (23) and, hence, must be retained. This fact is mathematically explicit when comparing the first term to the second term on the right-hand side of Equation (36).

For a smaller depth parameter $h = 0.1430$, the solution of Equation (36) yields

$$(\Delta z)_{\rm TGWE} = -2.06\ {\rm km},$$

while the solution of the TWE (3) gives

$$(\Delta z)_{\rm TWE} = -0.56\ {\rm km}$$

for exactly the same model and parameter values. In this case, since the zonal winds are not as deep, the difference between $\rho'_{\rm TGWE}$ and $\rho'_{\rm TWE}$ is expected to be less pronounced,

$$\Delta_{\rm diff} = \frac{\|\rho'_{\rm TGWE}(\boldsymbol{r}) - \rho'_{\rm TWE}(\boldsymbol{r})\|_2}{\|\rho'_{\rm TWE}(\boldsymbol{r})\|_2} = 39.75\%.$$

Again, the solution of the TWE (3) measured by the size of $\Delta z$ is substantially different from that of the TGWE (23): $(\Delta z)_{\rm TGWE}$ is more than 300% larger than $(\Delta z)_{\rm TWE}$ even for the small depth parameter $h = 0.1430$.

A unique feature of the TGWE (23) is that it contains the Green's function $1/|\boldsymbol{r} - \tilde{\boldsymbol{r}}|$ in its integrand and, consequently, the numerical convergence of its solution can be slow. It is found that, even for the large-scale wind $U_{\rm asym}(r, \theta)$ given by Equation (34), a high-resolution grid system is required to represent the converged solution of Equation (36). The behavior of the slow numerical convergence is shown in Table 1 for $N = 50$. For example, we obtain $(\Delta z) = -2.34$ km with $N_\xi \times N_\theta = 160 \times 320$ and $h = 0.1430$, while Equation (36) yields $(\Delta z) = -2.06$ km when $N_\xi \times N_\theta = 220 \times 440$. The estimated converged value for sufficiently large $N_\xi \times N_\theta$ is $(\Delta z)_{h=0.1430} \approx -2.00$ km. Moreover, it is found that the spectral truncation parameter $N$ in Equation (36) is less significant: the truncation at $N = 50$ seems sufficiently large for this solution because $N = 100$ gives rise to nearly the same solution.

### 4.2. Equatorially Symmetric Zonal Winds

Second, we consider a simple equatorially symmetric wind $U_{\rm sym}(r, \theta)$ in the form

$$U_{\rm sym}(r, \theta) = U_0 \left(\frac{r \sin\theta}{R_{\rm s}}\right)^2 e^{-\frac{R_{\rm s}-r}{hR_{\rm s}}}, \tag{37}$$

where $U_0$ and $h$ remain the same as in Equation (34) and

$$U_{\rm sym}(r, \theta) = U_{\rm sym}(r, \pi - \theta),$$

such that the wind-driving term can be evaluated analytically. Using the hydrostatic density $\rho_{\rm static}(r)$ given by Equation (31) and the zonal wind profile (37), we find that the analytic expression for the wind-driving term in the TWE (3) or the TGWE (23) is

$$\begin{aligned} &2\Omega \int_{\pi/2}^{\theta} \left[\cos\tilde{\theta}\frac{\partial}{\partial r} - \frac{\sin\tilde{\theta}}{r}\frac{\partial}{\partial\tilde{\theta}}\right]\left(\rho_{\rm static} U_{\rm sym}\right) d\tilde{\theta} \\ &= \frac{\Omega^2 \rho_{\rm c}}{150\pi} e^{-\frac{\pi-\xi}{h\pi}} \\ &\quad \times \left(-\sin\xi + \xi\cos\xi + \frac{1}{h\pi}\xi\sin\xi\right)\sin^3\theta. \end{aligned} \tag{38}$$

Using the analytic expression (38), the numerical form of the TGWE (26) for the equatorially symmetric zonal wind becomes

$$\begin{aligned} &\frac{\Omega^2}{600\pi^2 G} e^{-\frac{\pi-\xi_i}{h\pi}} \\ &\quad \times \left(1 + \frac{1}{h\pi}\frac{\xi_i \sin\xi_i}{\xi_i\cos\xi_i - \sin\xi_i}\right)\xi_i^3 \sin^3\theta_j \\ &= \rho'_{ij} - \frac{1}{2}\sum_{l=1}^{N_\xi}\sum_{m=1}^{N_\theta} \sin\tilde{\theta}_m \rho'_{lm} \Delta\theta w_\theta \tilde{\xi}_l^2 \Delta\xi w_\xi \\ &\quad \times \sum_{n=0}^{N} f_n\left(\xi_i, \tilde{\xi}_l\right) P_n\left(\cos\theta_j\right) P_n\left(\cos\tilde{\theta}_m\right) \end{aligned} \tag{39}$$

for $i = 1, 2, 3, \cdots, N_\xi$ and $j = 1, 2, 3, \cdots, N_\theta$. After obtaining the density anomaly $\rho'$ from Equation (39), we can compute the gravitational coefficients $J_n$. Since it is anticipated that the large-scale $U_{\rm sym}(r, \theta)$ given by Equation (37) would primarily induce the lowermost order gravitational coefficients, we concentrate on the lowermost coefficient $J_2$ (note that $J_2^{\rm static} = 0$; thus, $J_2 = \Delta J_2^{\rm dyn}$ in spherical geometry) calculated

by performing the integration

$$J_2 = -\frac{2\pi\mathcal{L}^3}{M\pi^2} \times \int_0^{\pi}\int_0^{\pi} \tilde{\xi}^4 P_2(\tilde{\theta})\rho'(\tilde{\xi},\tilde{\theta})\sin\tilde{\theta}\, d\tilde{\theta}\, d\tilde{\xi},$$

where $\xi = 0$ (or $r = 0$) in this case represents the center of mass as well as the center of figure.

As in the previous antisymmetric case, we also consider two different depth parameters $h = 1.1430$ and $h = 0.1430$ in the equatorially symmetric zonal wind $U_{\rm sym}(r, \theta)$ given by Equation (37). For a large depth parameter $h = 1.1430$, the solution of Equation (39) using the parameters of the generic object yields

$$(J_2)_{\rm TGWE} = 1.553 \times 10^{-4},$$

while the solution of the TWE (3) gives

$$(J_2)_{\rm TWE} = 0.874 \times 10^{-4}$$

for exactly the same model and parameter values. The difference $\Delta_{\rm diff}$ between $\rho'_{\rm TGWE}$ and $\rho'_{\rm TWE}$ is

$$\Delta_{\rm diff} = \frac{\|\rho'_{\rm TGWE}(\boldsymbol{r}) - \rho'_{\rm TWE}(\boldsymbol{r})\|_2}{\|\rho'_{\rm TWE}(\boldsymbol{r})\|_2} = 101.43\%.$$

Evidently, this large difference between the solutions of Equations (3) and (23) is again a direct consequence of the gravitational perturbation term neglected in the TWE (3). It reinforces the view that the TWE (3) cannot generally provide a reasonable approximation to the TGWE (23).

In the case $h = 0.1430$ with the zonal flow concentrated more in the outer layer of the planet, the solution of Equation (36) yields

$$(J_2)_{\rm TGWE} = 5.00 \times 10^{-5}$$

while the solution of the TWE (3) gives

$$(J_2)_{\rm TWE} = 3.17 \times 10^{-5}$$

for exactly the same model and parameter values. It is expected that, when the zonal winds become sufficiently shallow (this point will be discussed further in Section 5), the difference between $\rho'_{\rm TGWE}$ and $\rho'_{\rm TWE}$ would be less pronounced. The smaller depth parameter $h = 0.1430$ gives

$$\Delta_{\rm diff} = \frac{\|\rho'_{\rm TGWE}(\boldsymbol{r}) - \rho'_{\rm TWE}(\boldsymbol{r})\|_2}{\|\rho'_{\rm TWE}(\boldsymbol{r})\|_2} = 53.35\%.$$

In conclusion, the solutions of the TWE (3), measured by the size of the gravitational coefficient $J_2$, are substantially different from those of the TGWE (23).

The numerical convergence for the equatorially symmetric solution (39) is much faster. For example, we obtain $J_2 = 5.0014 \times 10^{-5}$ when $N_\xi \times N_\theta = 80 \times 160$ with $N = 50$ and $h = 0.1430$, while the higher resolution $N_\xi \times N_\theta = 160 \times 320$ yields $J_2 = 5.0013 \times 10^{-5}$. Moreover, the convergence with increasing $N$ in Equation (39) is also satisfactory. For example, using the higher resolution with $N_\xi \times N_\theta = 160 \times 320$ and $N = 100$, the numerical solution of Equation (39) leads to $J_2 = 5.0014 \times 10^{-5}$.

## 5. SUMMARY AND REMARKS

The present study shows that the TWE (3)—which correctly relates the vertical shear of a flow to the horizontal density gradient in the thin atmosphere of the Earth—is incorrect for the purpose of computing the gravitational signature of a giant gaseous planet caused by the zonal winds in its deep interior. This is because an extra term representing the concomitant gravitational perturbation $\boldsymbol{g}'$ produced by the density anomaly $\rho'$ is of the same order of magnitude and, hence, must be retained, leading to the TGWE (23). Since the TGWE represents a two-dimensional kernel integral equation with the Green's function in its integrand, it is much more difficult to solve even in spherical geometry. An extended spectral method, represented by Equation (26) for a system of the $N_\xi \times N_\theta$ equations, is proposed to solve the system for determining the density anomaly $\rho'$. Using simple analytic profiles for both the zonal winds and the hydrostatic solution, we then apply the method to a generic gaseous object whose main parameter values are guided by the parameters of Jupiter. We have demonstrated that the solutions of the TGWE (23) are substantially different from those of the TWE (3) and that the TWE, in general, cannot provide a reasonable approximation to the TGWE.

There exist, however, two special circumstances in which the kernel integral in the TGWE (23) can be neglected and, consequently, the TWE (3) provides a good approximation to the TGWE (23). The first circumstance is when the interior fluid of a planet is weakly compressible everywhere, i.e.,

$$\left|\frac{\mathcal{L}}{\rho_{\rm static}(r)}\frac{d\rho_{\rm static}(r)}{dr}\right| \ll 1 \quad \text{in} \quad 0 < r < R_{\rm s}.$$

However, this case does not represent the typical interior of a giant gaseous planet like Jupiter, which is believed to be strongly compressible. The second circumstance is when the zonal winds $U$ and the corresponding wind-induced density perturbation $\rho'$ are primarily confined within a very thin outer layer defined by $(R_{\rm s} - \epsilon) \leqslant r \leqslant R_{\rm s}$ with $0 < (\epsilon/R_{\rm s}) \ll 1$. In this case, the TGWE (23) becomes

$$\begin{aligned} &2\Omega\int_{\pi/2}^{\theta}\left[\cos\tilde{\theta}\frac{\partial}{\partial r} - \frac{\sin\tilde{\theta}}{r}\frac{\partial}{\partial\tilde{\theta}}\right]\left(\rho_{\rm static}U\right)d\tilde{\theta} \\ &= \frac{g_{\rm static}(r)}{r}\rho'(r,\theta) - \frac{2\pi G q(r)}{r} \\ &\times \int_0^{\pi}\int_{(R_{\rm s}-\epsilon)}^{R_{\rm s}} \frac{\tilde{r}^2\rho'(\tilde{r},\tilde{\theta})}{|\boldsymbol{r}-\tilde{\boldsymbol{r}}|}\sin\tilde{\theta}\, d\tilde{r}\, d\tilde{\theta} \\ &= \frac{g_{\rm static}(r)}{r}\rho'(r,\theta) - O(\epsilon/R_{\rm s}), \end{aligned}$$

which represents the standard TWE widely used in atmospheric dynamics where the gravitational force $g_{\rm static}(r)$ in the thin layer $(R_{\rm s} - \epsilon) \leqslant r \leqslant R_{\rm s}$—which mainly originates from the deep mantle and core—may be regarded as being constant. However, this case represents an uninteresting trivial case not

only because we are concerned with how a deep wind induces an externally measurable gravitational signature but also because it is obvious that $\Delta J_n^{\rm dyn} \to 0$ when $(\epsilon/R_{\rm s}) \to 0$.

With the correct TGWE (23) for computing the external gravitational signature induced by deep zonal winds, we still face two major unresolved difficulties. First, the TGWE (23) is only valid for spherical geometry and cannot be readily modified for a rapidly rotating gaseous planet that departs significantly from a spherical shape. This difficulty is marked by the feature that the latitudinal components, $\hat{\boldsymbol{\theta}} \cdot \boldsymbol{g}_{\rm static}$ and $\hat{\boldsymbol{\theta}} \cdot \boldsymbol{\nabla} \rho_{\rm static}$, become non-negligibly small in non-spherical geometry. Second, the numerical convergence of the system (26), a consequence of the nature of the Green's function $1/\left|\boldsymbol{r} - \tilde{\boldsymbol{r}}\right|$ in the integrand of Equation (23), is usually slow. Even with a spatially simple, smooth profile of the zonal winds $U$, we have encountered some numerical difficulties in computing a well-converged solution for the system (36), as shown in Table 1. This is likely to cause more computational difficulties when calculating, via the TGWE (23), the gravitational signature of a real giant planet using the spatially complicated profile of the zonal winds. Interpretation of high-precision gravitational measurements for Jupiter and Saturn—which requires taking into account the full effect of rotational distortion for $J_n^{\rm static}$ and computing the wind-induced $\Delta J_n^{\rm dyn}$ in non-spherical geometry—remains a challenging task that defies a simple solution.

K.Z. is supported by Leverhulme Research Project Grant RPG-2015-096 and the HKRGC grant (Project 14306814), D.K. is supported by the NSFC under grant 11473014, and G. S. is supported by the National Science Foundation under grant NSF AST-0909206. The computation made use of the high-performance computing resources in the Core Facility for Advanced Research Computing at Shanghai Astronomical Observatory, Chinese Academy of Sciences.

## REFERENCES

Busse, F. 1976, Icar, 29, 255
Chandrasekhar, S. 1933, MNRAS, 93, 390
Guillot, T., & Morel, P. 1995, A&AS, 109, 109
Holton, J. R. 2004, An Introduction to Dynamic Meteorology (New York: Academic)
Hubbard, W. B. 1999, Icar, 137, 357
Hubbard, W. B. 2013, ApJ, 768, 43
Kaspi, Y. 2013, GeoRL, 40, 676
Kaspi, Y., Hubbard, W. B., Showman, A. P., & Flierl, G. R. 2010, GeoRL, 37, L01204
Kaspi, Y., Shaowman, A. P., Hubbard, W. B., Aharonson, O., & Helled, R. 2013, Natur, 497, 344
Kong, D., Liao, X., Zhang, K., & Schubert, G. 2013a, Icar, 226, 1425
Kong, D., Liao, X., Zhang, K., & Schubert, G. 2014, ApJL, 791, L24
Kong, D., Zhang, K., & Schubert, G. 2012, ApJ, 748, 143
Kong, D., Zhang, K., Schubert, G., & Anderson, J. 2013b, ApJ, 763, 116
Liu, J., Schneider, T., & Kaspi, Y. 2013, Icar, 224, 114
Zhang, K. 1992, JFM, 236, 535
Zhang, K., & Schubert, G. 1996, Sci, 273, 941
Zharkov, V. N., & Trubitsyn, V. P. 1978, in Physics of Planetary Interiors, ed. W. B. Hubbard (Tucson, AZ: Pachart Publishing House)